Practical Implementation of Broadband Diffractive Optical Elements

Junoh Choi, Alvaro A. Cruz-Cabrera, Anthony Tanbakuchi
Sandia National Laboratories, PO Box 5800, MS 0406, Albuquerque, NM 87185

ABSTRACT

Diffractive optical elements (DOEs), with their thin profile and unique dispersion properties, have been studied and utilized in a number of optical systems, often yielding smaller and lighter systems. Despite the interest in and study of DOEs, the application of DOEs has been limited to narrow spectral bands. This is due to DOEs depths, which are optimized for optical path differences of only a single wavelength, consequently leading to rapid decline in efficiency as the working wavelength shifts away from the design wavelength. Various broadband DOE design methodologies have recently been developed that improve spectral diffraction efficiency and expand the working bandwidth of diffractive elements. Two such extended bandwidth diffractive designs have been modeled and fabricated. The diffraction efficiency test result for one broadband DOE design is presented.

Keywords: Diffractive optical element, broadband diffractive

1. INTRODUCTION

Diffractive optical elements are components that redirect light by altering the wavefront of subsections of a beam and stitching them as the wavefront propagates away from the device. The stitching occurs because the optical path difference imparted by each subsection is an integer multiple of the working wavelength. The zone spacing of a DOE can be designed to add a focusing or even an aspheric term to an incident wavefront. The depths of DOEs are much smaller than refractive element sags and lead to thinner profile components. However, although DOEs are thinner than the traditional refractive lenses, the use of DOEs has been limited to narrow spectral bands due to rapid loss of diffraction efficiency at non-design wavelengths. Recent efforts[1,2] to expand the working spectral bandwidth of diffractive elements have led to design methodologies that improve the diffraction efficiency over a larger range of wavelengths. Multi-layer diffractive and the harmonic, or multi-order, diffractive designs are two examples of such broadband diffractive designs. Spectral transmission is an important parameter that needs to be understood for a broadband optical system and if a broadband DOE is to be incorporated into a broadband system, then the DOE's spectral diffraction efficiency will need to be well characterized.

In this paper we present results from design, efficiency modeling, and fabrication of the two aforementioned broadband diffractive element designs. The DOEs were fabricated with fused silica and calcium fluoride by grayscale lithography and diamond turning, respectively. We also present results from spectral diffraction efficiency measurements of the harmonic diffractive element.

2. DESIGN AND MODELING

Design considerations for a DOE are in some aspects similar to those of a traditional lens in that typical raytrace software can be used to design a DOE's optical power, clear aperture, and the material. These typical optical parameters then translate to zone spacings, and number of zones in a clear aperture for a DOE. Another parameter that needs to be modeled and specified for a DOE is the step height of the diffraction surface that determines the diffraction efficiency of the designed orders. We modeled the spectral diffraction efficiencies of the two broadband design methods to determine the desired depths of the DOE designs. Also, to ensure manufacturability of the designed DOEs, we performed a survey of the manufacturing industry and put together a loose set of guidelines – due to lack of a clear set of limitations – for fabrication limits for lithography on fused silica and diamond turning calcium fluoride.

Micromachining and Microfabrication Process Technology XVIII, edited by Mary Ann Maher, Paul J. Resnick,
Proc. of SPIE Vol. 8612, 86120G · © 2013 SPIE · CCC code: 0277-786X/13/$18 · doi: 10.1117/12.2013204

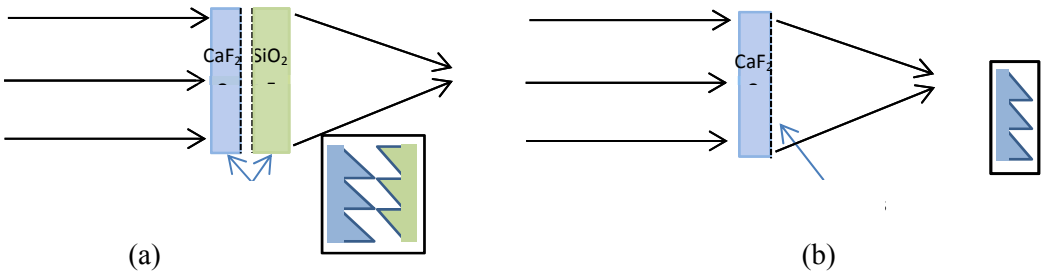

Figure 1. (a) Depicts the "efficiency achromatized"(multi-layer) DOE and (b) depicts the multi-order DOE.

2.1 Efficiency model of multi-order or harmonic diffractive optical element

The multi-order DOE does not actually broaden the efficiency at a given wavelength but provides multiple wavelengths where the efficiency is high with a diffraction angle identical to the diffraction angle at the design wavelength. This device differs from the multi-layer DOE by using only one material. Its depths are integer multiples of the optimized depth for a conventional diffractive:

$$d_h = p\frac{\lambda_0}{n_0 - 1} \tag{1}$$

Where p is an integer that denotes the harmonic (p is 1 in standard DOEs), λ_0 is the design wavelength, and n_0 is the refractive index at the design wavelength. By increasing the depth by integer multiples the harmonic DOE allows adjacent orders to provide near unity efficiencies at different wavelengths. The efficiencies are calculated using reference 2:

$$\eta = \sum e^{-i\pi(\alpha p - m)} sinc(\alpha p - m) e^{\left(\frac{-i\pi m r^2}{p\lambda_0 F_0}\right)} \quad and\ \alpha = \frac{\lambda_0}{\lambda}\left(\frac{n(\lambda)-1}{n(\lambda_0)-1}\right), \tag{2}$$

where α is the 2π phase delay for wavelengths other than the intended wavelength, m is the diffraction order and F_0 is the focal length for the design wavelength. Figure 2 shows a 2D description of the efficiencies of the DOE. White is efficiency close to 1 and black is zero efficiency. The y-axis is the wavelength range for the analysis of the DOE, and the x-axis is the diffractive order. Notice that at 0.55μm the utilized order is 20. This is the case we are trying to fabricate with a depth of 25.32μm and a minimum zone width to depth ratio of 22.48:1, which is well within the advised fabrication limits of current fabrication methods.

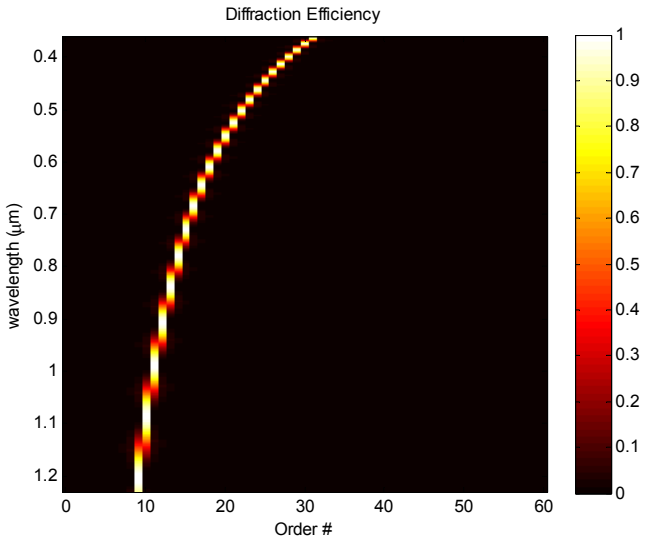

Figure 2. Shows diffraction efficiency of the multi-order DOE as function of the order number (x-axis) and its wavelength (y-axis). White is an efficiency of 1 and black is an efficiency of 0. The graph shows that as the wavelength gets shorter the order numbers with high efficiency increase.

Another aspect that needs to be addressed in this type of device is the sparsity of high efficiency orders; see Figure 3(a) for p= 20. With deeper structures we can increase the number of higher efficiency orders; see Figure 3(b) for p= 40. These two figures show the efficiency (y-axis) for each order (each one has a different color) versus wavelength (x-axis). The example in Figure 3(b) show that the orders with high diffraction efficiency are more closely packed when the design uses more harmonics, and consequently the device gets deeper.

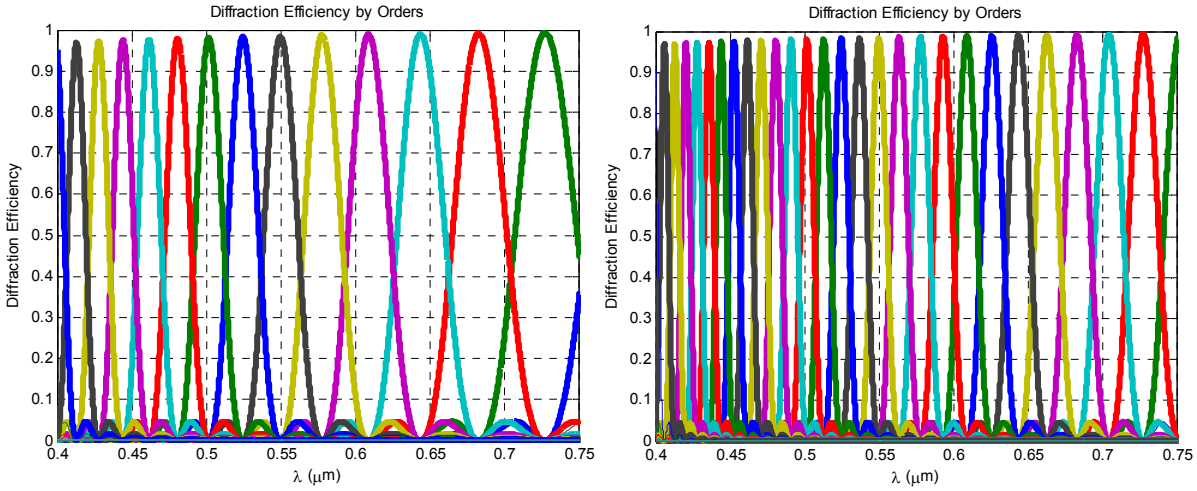

Figure 3. Graph shows the efficiency of DOE for all possible orders and no limitation in acceptance angle. Panel (a) shows the case where p= 20 is used to define an etch depth of 25.31μm, but providing ample separation between the peak efficiency of each order, and where the diffraction angles are close but not identical due to dispersion. Panel (b) shows the case where p= 40 is used to define an etch depth of 50.61μm, while providing a closer separation between the peak efficiency of the orders. Each color is an order that peaks its efficiency at different wavelength.

It can also be determined from the grating equation $sin\theta = p\,{}^{\lambda}/_{\Lambda}$, (where Λ is the period) that each order at its peak efficiency will diffract at the same angle as the other orders. Figure 4(a) shows that behavior for a material without dispersion. However with real material, dispersion needs to be accounted as the focal point changes with the order, see Figure 4(b).

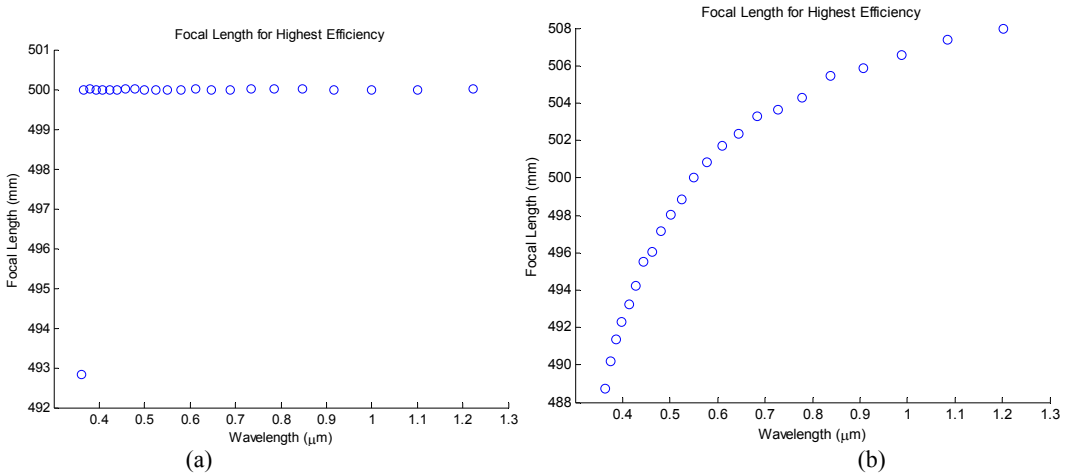

Figure 4. Focal length for (a) an ideal case where there is no material dispersion and (b) with measured dispersion, in this case of calcium fluoride. Each of the dots in the curves corresponds to the highest efficiency of an order. The leftmost point from panel (a) is an artifact of the calculation, as it is at the boundary of the measured dispersion for calcium fluoride.

A perfect theoretical harmonic DOE will restrict diffraction angle to the calculated diffraction angle, and that will limit the amount of light being accepted; see Figure 5(a). If the acceptance angle is wider, then the system will seem to provide a better efficiency response; see Figures 5(b) and (c). However, the spot size at the focal plane will be degraded.

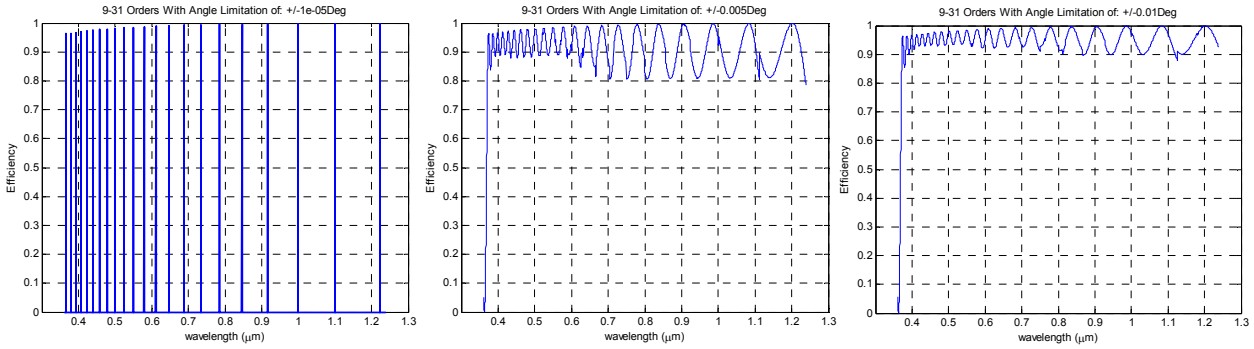

(a) (b) (c)

Figure 5. Panel (a) shows the DOE efficiency for a 20 harmonic DOE in the visible range with limitations in the acceptance angle of +/- 0.00001 Degrees (this number is used for demonstration purposes). Panel (b) shows the same DOE but restricting its acceptance angle to +/- 0.005 Degrees. Panel (c) shows a restriction to an acceptance angle of +/-0.01 Degrees.

2.2 Efficiency model of multi-layer diffractive optical element

Unlike the MOD design, the multi-layer diffractive design broadens the spectral diffraction efficiency by using two materials with different dispersion properties. Each substrate has a deep etch diffractive on one side, facing each other where the two kinoforms have complementary surface profiles; see Figure 1(a). The addition of a second material provides two additional degrees of freedom - the depth of the second kinoform and its dispersion - that modify the spectral efficiency of the combined system to provide two peaks. The phase change induced by the two complementary kinoforms is[1]:

$$\Phi(\lambda) = \frac{2\pi h_1}{\lambda}(n_1(\lambda) - 1) - \frac{2\pi h_2}{\lambda}(n_2(\lambda) - 1), \quad (3)$$

where n_1 and n_2 are the refractive indices of the materials, h_1 and h_2 are the depths of the respective kinoforms, and the λ is the wavelength. This equation assumes that the devices are working at scalar regimes (the periods are at least 10 times larger than the working wavelength).

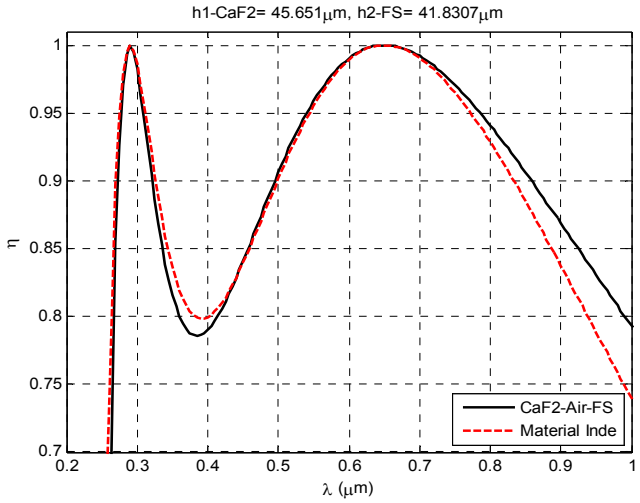

Figure 6. Curves show generic prediction of efficiency for EA-DOE with two design wavelengths of 0.290μm and 0.65μm. This design solution clearly shows the two efficiency peaks.

Figure 6 shows an example of a non-optimal but illustrative design showing two peaks in the diffraction efficiency of the multi-layer element. The red curve is the calculated efficiency using the dispersion of fused silica and calcium fluoride, the black curve comes from a derived equation[1] that is independent of the material. The example in Figure 6, however, requires diffractive elements with depths greater than 40 microns. With the zone widths for the particular design we were considering, the depth did not yield a manufacturable design. We modified the design to come as close to the current fabrication limitations as possible which resulted in the diffraction efficiency curve to have a closely placed peak wavelengths at 0.35um and 0.4um. See Figure 7.

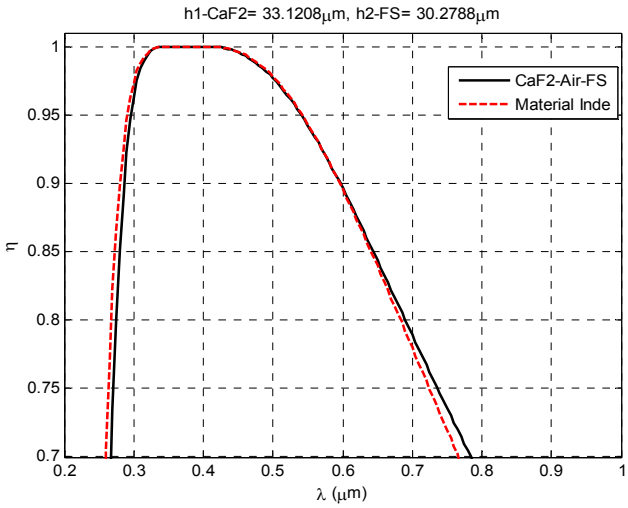

Figure 7. Prediction of the efficiency response of the EA-DOE. The red curve is the calculated response using the dispersion of fused silica and calcium fluoride, the black curve comes from the equation that is independent to material. The flat top is the location for the two wavelength peak designs of 0.35μm and 0.4μm.

This narrow band was selected for the fused silica substrate etch-depth of 30.28μm and 33.12μm for calcium fluoride. The minimum zone width and the step height ratio of the final multi-layer DOE design had a ratio of 7.6:1 for fused silica, a 6.97:1 ratio for calcium fluoride.

3. FABRICATION

One component of the multi-layer diffractive was fabricated using grayscale lithography with fused silica as the substrate material. The complementary diffractive component as well as the harmonic DOE design were diamond turned on calcium fluoride. The as-built multi-layer DOE had a clear aperture diameter of 14mm and the harmonic DOE had a clear aperture diameter of 20mm. After receiving the manufactured components, they were examined and the 1-D surface profiles were compared to their respective design values. Results from the surface profile measurements with a Dektak profilometer of a lithographically etched diffractive and a diamond-turned diffractive are shown below. It should be noted that the profilometry was done with a probe tip with a diameter of 2 microns and the diamond turning tool tip had a diameter of 25 microns. Also, the results shown are for two different diffractive designs where the step height and the zone widths, as well as the clear aperture and the total number of zones, differ.

3.1 Surface profile of diamond-turned component

The surface profile shown in Figure 8 is of the diamond turned component designed as the harmonic DOE. Some of the fabrication errors observed are the step height error, the zone spacing error, and the zone transition error. Figure 8 shows the surface profile comparison of the as-built against the design. The error in the step height in the central zone is approximately 4%. The zone depth as well as the zone spacing shows radial variation where the error appears to slightly grow with the radius. At the location of the last zone, the depth error is as great as 10% and the zone spacing error is approximately 1 micron.

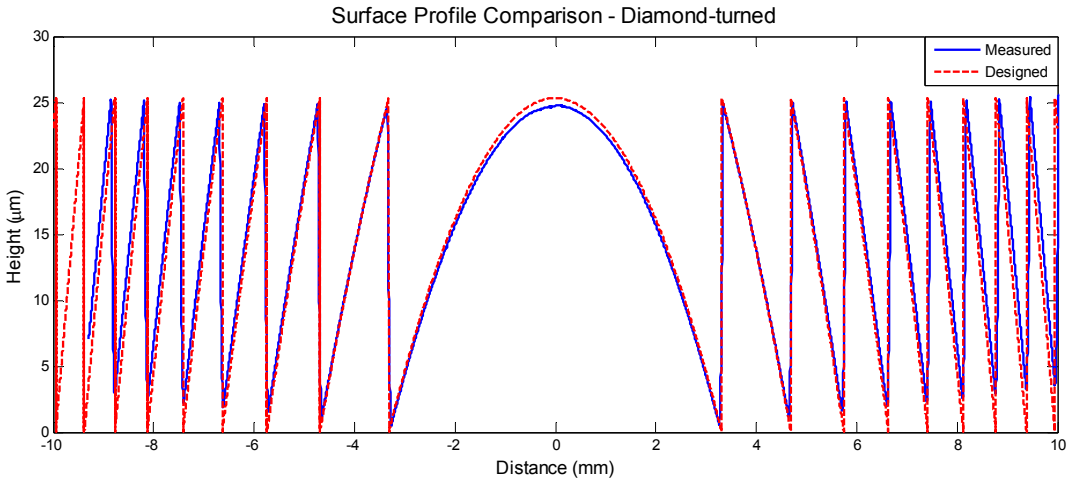

Figure 8. Surface profile of the diamond-turned harmonic DOE in calcium fluoride

Plots included in Figure 9 show surface roughness in the central zone of the diamond-turned DOE and a region of a zone transition. As expected, the zone transition shows sloped boundary with a rounded corner.

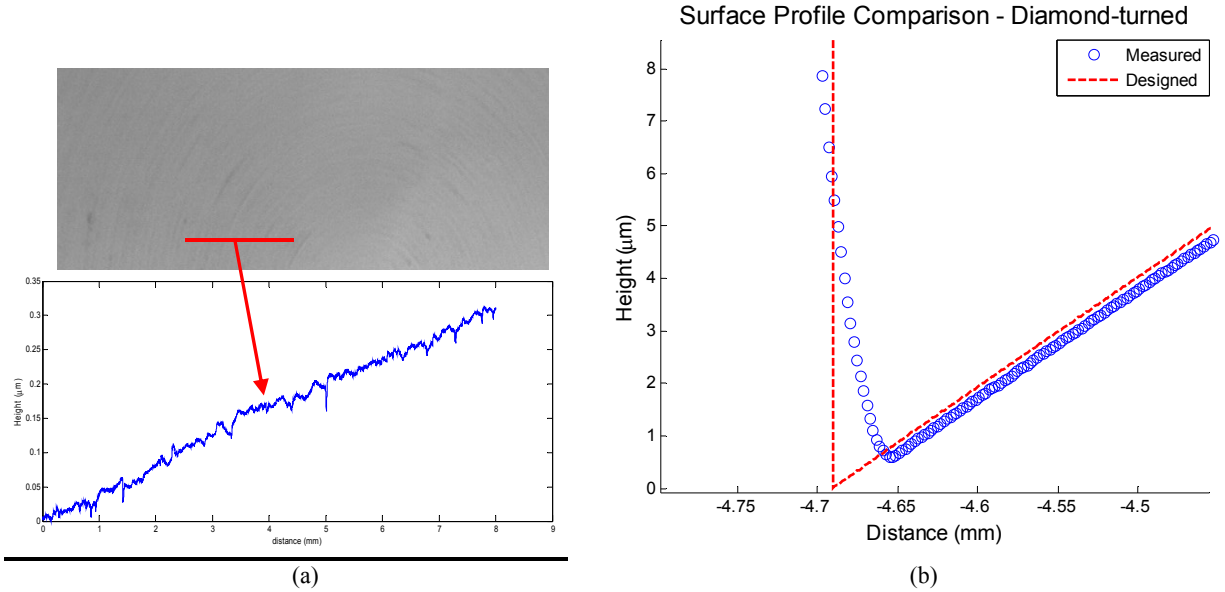

(a) (b)

Figure 9. Results from surface profilometry of the diamond-turned diffractive element showing (a) surface roughness, and (b) zone transition error

The surface profilometry data was used to calculate the RMS surface error of the diamond-turned DOE for the central zone region. The RMS surface roughness was calculated from the profile data after removing the surface figure with a best-fit 8th order polynomial from the measured data. Close-up view of the data from the central zone clearly captures the slight discontinuity at the center of the component. See Figure 10. The RMS surface error calculated from the data is 0.014 microns. Using the following approximation for total integrated scatter[3],

$$TIS \approx \left(\frac{2\pi\sigma\Delta n}{\lambda}\right)^2, \tag{4}$$

where σ is the RMS surface roughness, Δn is the difference in refractive indices, the estimated scatter from surface roughness is about 0.4% at 600nm and 0.31% at 700nm. It can be expected from the power spectral density plot in Figure 10(c) that most of that scatter will happen at small angles near the specular ray.

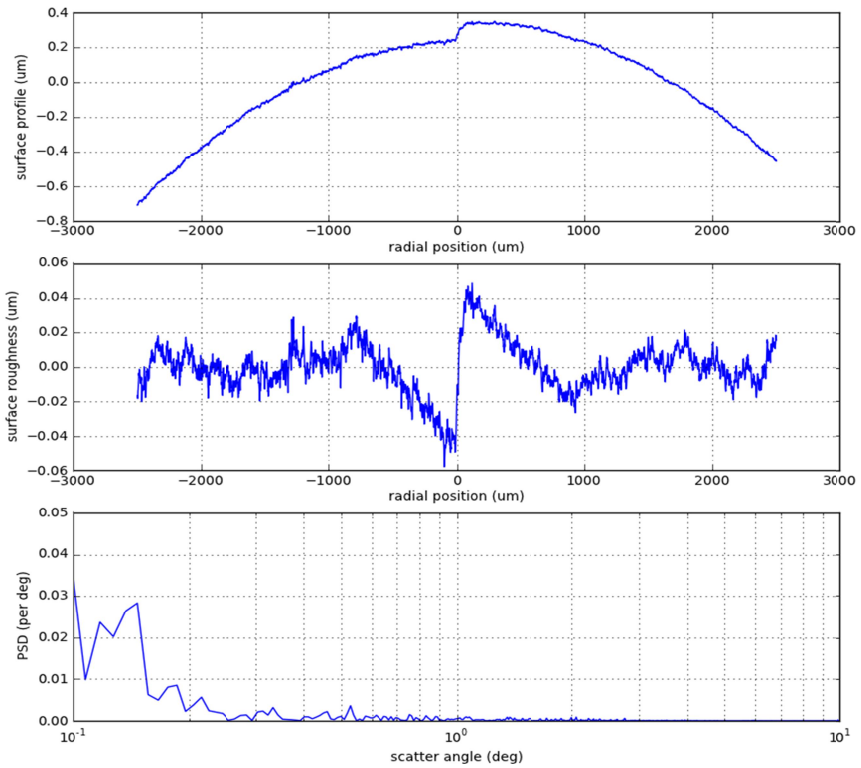

Figure 10. Results from surface profilometry of the diamond-turned diffractive element showing (a) surface profile, (b) surface roughness, and (c) power spectral density plot.

3.2 Surface profile of grayscale lithographed component

The grayscale diffractive element also showed some error in the etch depth which was measured at approximately 4% and as great as 8% near the edge of the clear aperture. Surface profile plots of the measured versus the design is shown in Figure 11. Errors in zone spacings are measured to be as great as 20nm.

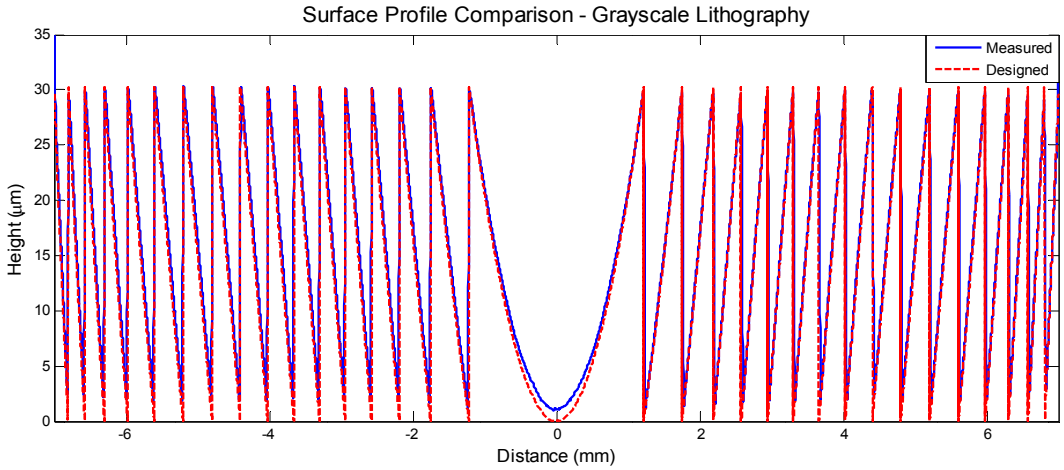

Figure 11. Surface profile of lithographically etched diffractive element.

An interesting feature that was captured during the inspection with the profilometer is the corrugation in the central zone of the element which we suspect is an artifact of the error present in the mask. An image of a region in the central zone is shown in Figure 12 (a) with a surface plot clearly depicting the linear features.

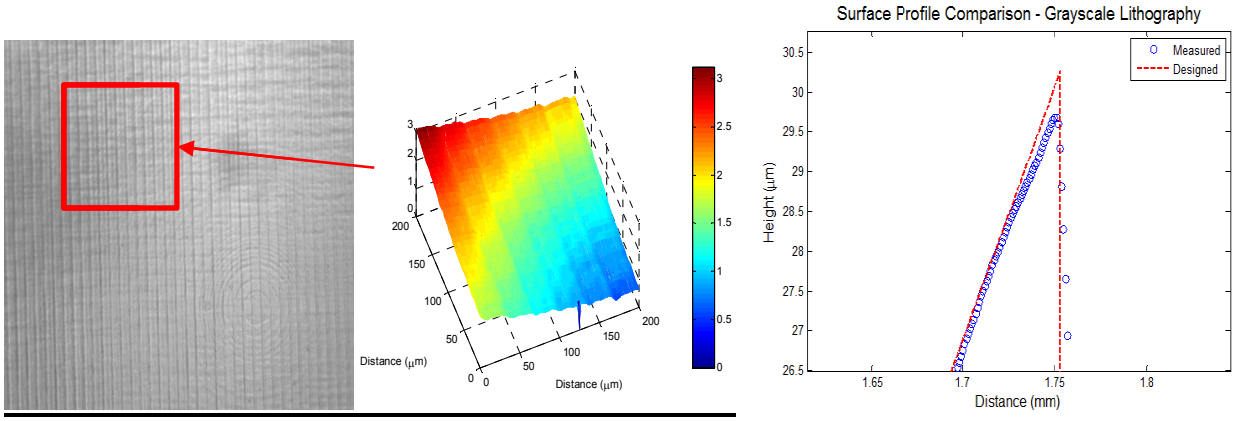

Figure 12. Results from the surface profilometry showing (a) corrugation in the central zone and (b) zone transition error.

Figure 13 shows a surface profile plot, a surface roughness plot, and a power spectral density. The surface roughness was calculated the same way it was done for the diamond-turned optic and the calculated RMS error was 0.038 microns for the lithographed component. From the RMS value, the estimated scatter is 3.3% at 600nm and 2.4% at 700nm. The power spectral density plot shows that the grayscale element will have scattered light that is mostly directed in angles near 1 degree and 2 degrees.

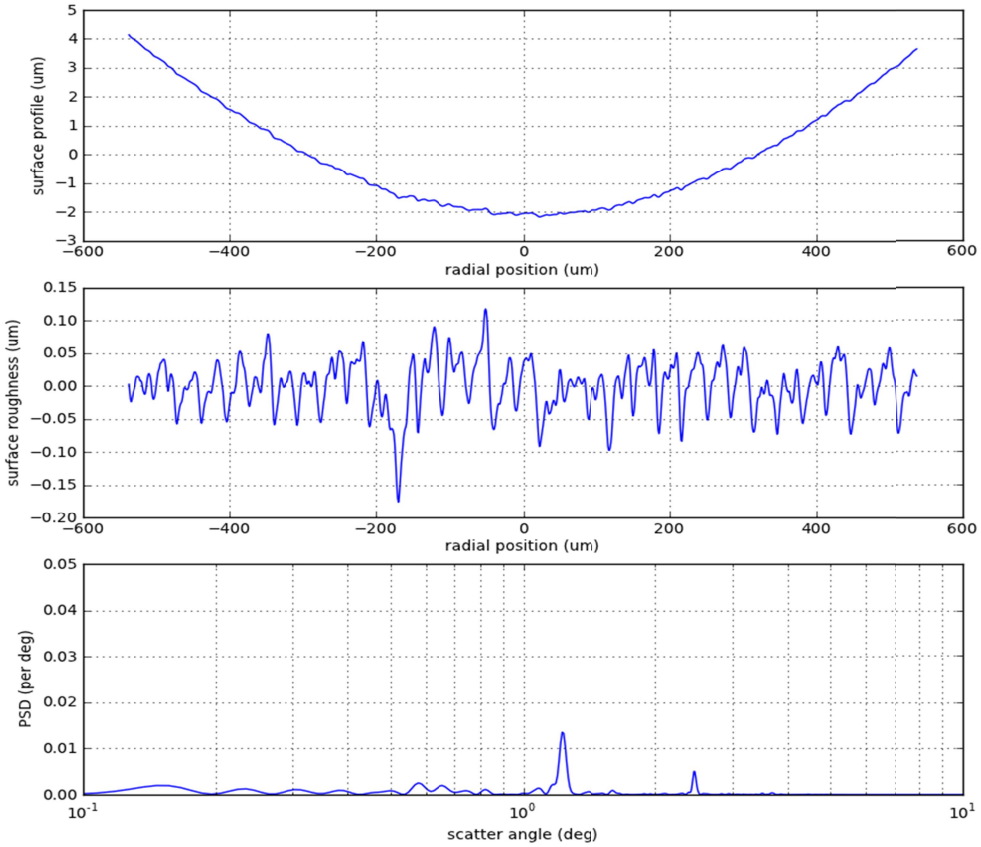

Figure 13. Results from surface profilometry of the lithographically etched component showing (a) surface profile, (b) surface roughness, and (c) power spectral density.

4. DIFFRACTION EFFICIENCY MEASUREMENTS

Transmittance is a property of a material defined as the fraction of the incident light that passes through the material. For a lens with focusing power, the transmittance of the lens material determines how much energy passes to the image plane and the aberration content of the lens governs how that energy is distributed. Diffraction efficiency of a DOE can be thought of in a similar manner. Diffraction efficiency of a DOE is the primary variable that determines how the incident energy is distributed in the image plane. For example, a DOE with high diffraction efficiency would have most of the incident energy fall in a focused spot like a refractive lens would do.

The designed harmonic DOE was an f/25 lens where optical modeling software, ignoring diffraction efficiency, simulated a diffraction limited performance. We identified Newport's SPX031 lens as a reference refractive lens with a comparable focal length lens and added an aperture to operate it at f/25. Both the harmonic DOE and the refractive lens were uncoated singlets. Our method of measuring the diffraction efficiency involved collimating a laser source and measuring power at the focal plane of the harmonic DOE. P_{in}/P_{out} ratio for the harmonic DOE was then normalized by the same P_{in}/P_{out} ratio measured with the reference refractive lens. We call this normalized ratio the measured diffractive efficiency in this paper. Figure 14 shows the layout of the optical bench test setup.

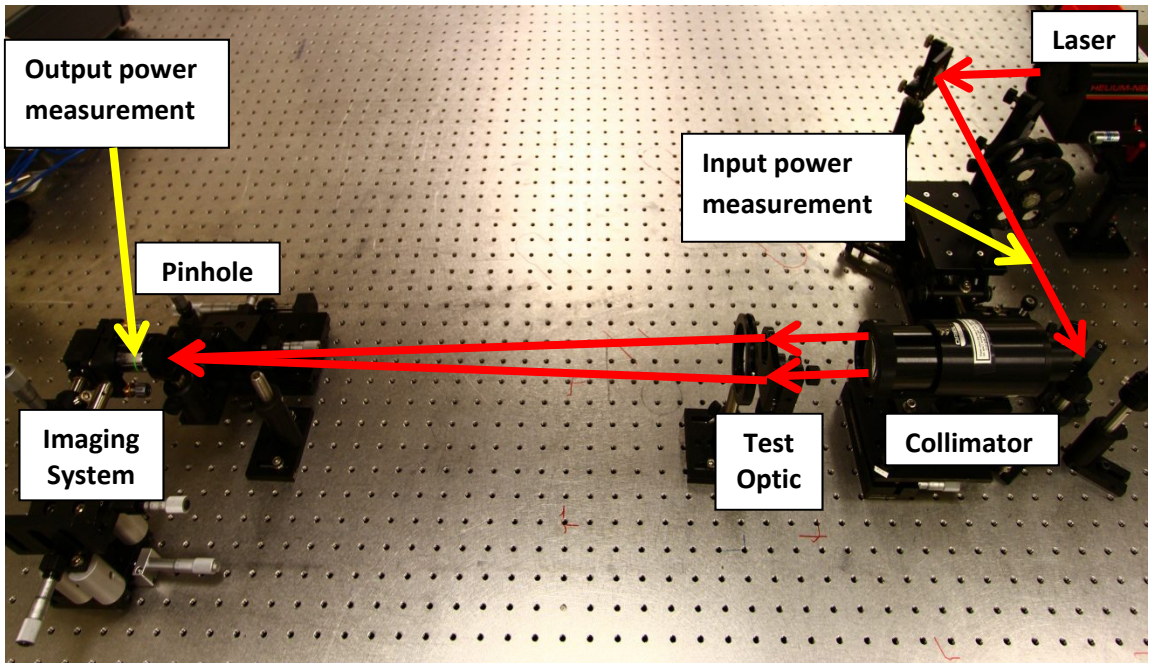

Figure 14. Layout of the experimental setup

Isolating power from the desired order from light from other orders was a critical step in these measurements. Both the harmonic DOE and the reference refractive lens were diffraction limited, so a pinhole was placed at the focal plane to select only the Airy disk diameter for the power measurements. As the point spread function and encircled energy plots in Figure 15 indicate, optical performance of the lenses is comparable. A pinhole with a diameter of 50 microns was selected to be used for these measurements.

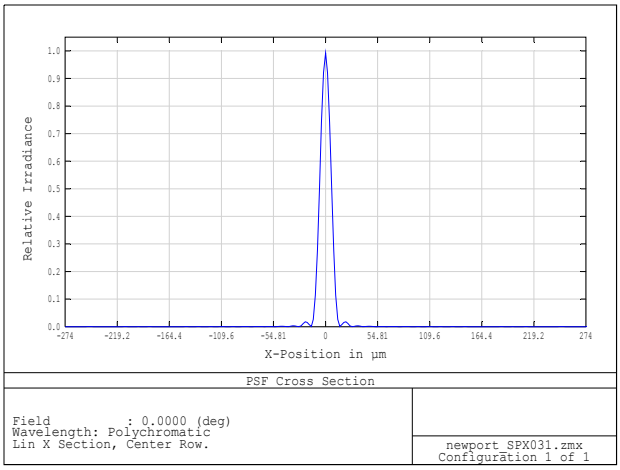

(a)

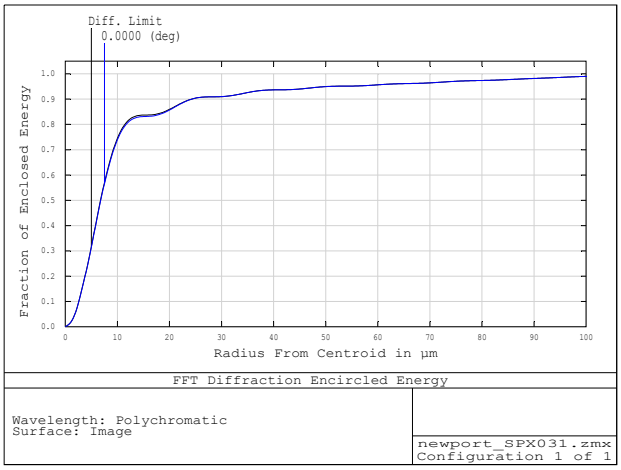

(b)

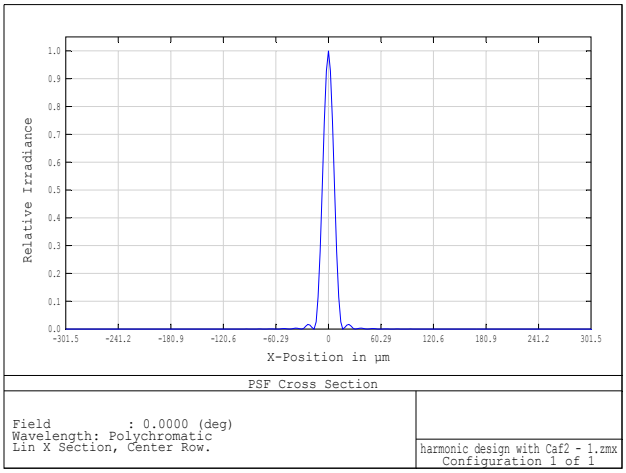

(c)

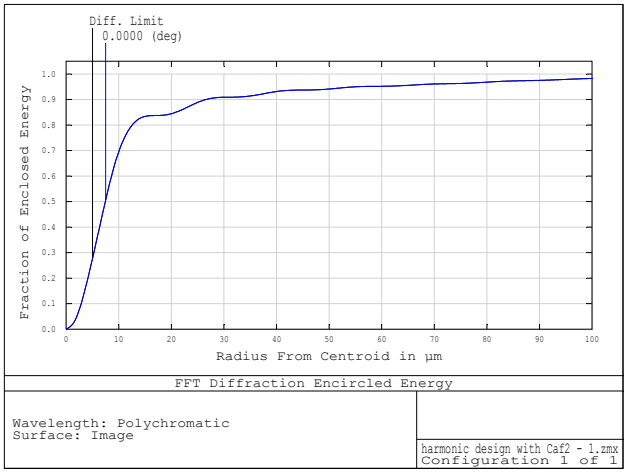

(d)

Figure 15. (a) Point spread function of the reference refractive lens, (b) Encircled energy plot of the reference refractive lens, (c) PSF of the harmonic diffractive lens, and (d) Encircled energy plot of the harmonic diffractive element.

Figure 16 shows sample images of the focused spot with the lenses and with the pinhole acting as a filter to filter out only the Airy disk diameter.

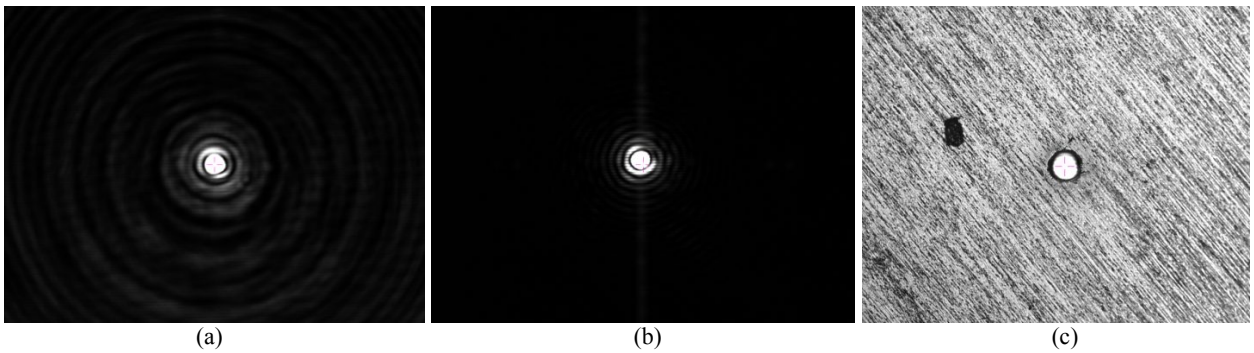

(a) (b) (c)

Figure 16. Image of the focused spot with (a) the harmonic diffractive lens at 810nm, (b) the reference refractive lens at 740nm, (c) with the 50 micron pinhole.

We used a tunable HeNe at wavelengths of 594nm, 604nm, 612nm, 633nm and a tunable Ti:Sapphire laser for measurements from 700nm to 1000nm in increments of 10nm. A plot of the measured diffraction efficiencies is shown in Figure 17 against the modeled efficiency curve. The measured efficiency peaks were about 90% and were all located near the expected wavelengths for wavelengths below 900nm. The troughs in the measured diffraction efficiency were around the 40%~50% mark in the same wavelength range. However, results for wavelengths between 900nm and 1000nm did not show noticeable peaks and the efficiencies were all generally low compared to results for wavelengths below 900nm.

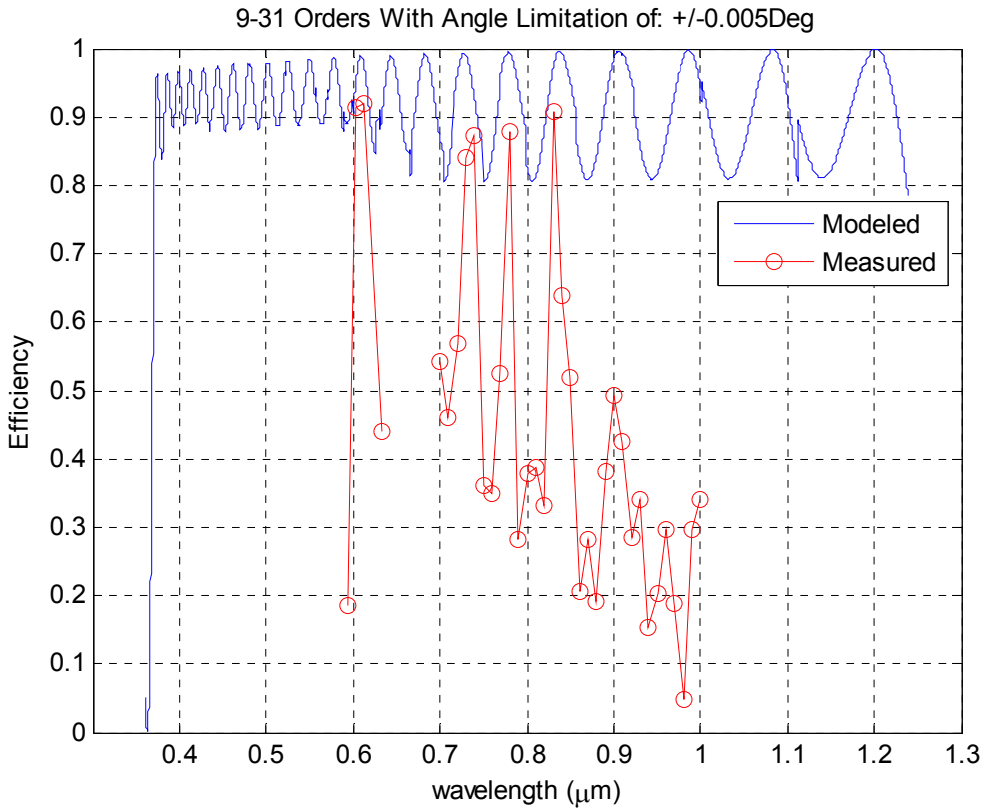

Figure 17. Plot of measured diffraction efficiency of the harmonic diffractive element. The measurement of the first group (0.594um to 0.633um) was done with a tunable HeNe laser while the second group (0.7um to 1.0um) was done with a tunable Ti:Sapphire laser.

One possible explanation for the disagreement in the 900nm-1000nm region could be the change in the coherence length of the laser and effects from interference. As is evident from Figure 18, a fringe pattern is present and more pronounced at 900nm than at lower wavelengths.

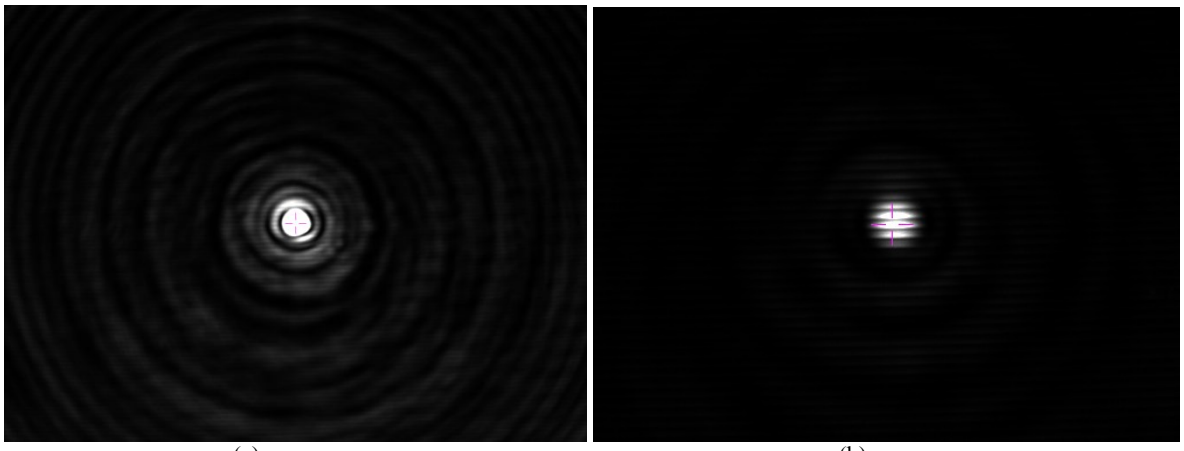

(a) (b)

Figure 18. Image of focused spot with the harmonic DOE at (a) 810nm, and at (b) 900nm

5. CONCLUSIONS AND FUTURE WORK

We have designed, fabricated, and tested two extended spectral efficiency diffractive elements. One design involved two complementary diffractive elements made with different materials and the other was a single component harmonic diffractive element. Both designs required deeper than conventional step heights approaching fabrication limitations for such designs using fused silica and calcium fluoride. The diffraction efficiency of the MOD lens was measured by comparing power at the focused spot against a reference refractive lens at various wavelengths. The results showed peak efficiency of approximately 90% and a low of about 50% within measured wavelengths below 900nm. Above 900nm however, the results were not in agreement with the predictions possibly due to fringes present at the focal plane where the powers were measured. The multi-layer diffractive design will be tested in the future in a similar manner to measure its spectral diffraction efficiency.

ACKNOWLEDGEMENT

Sandia is a multi-program laboratory operated by Sandia Corporation, a Lockheed Martin Company, for the United States Department of Energy under contract de-ac04-94al85000. This work was supported by Sandia National Laboratories lab directed research and development program.

REFERENCES

[1] Kleemann, B.H., Seesselberg, M., Ruoff, J., Design concepts for broadband high-efficiecy DOEs. *Journal of the european optical society - rapid publications 3*, 08015 (april 2008), 1-16.

[2] Morris, G.M., Faklis D., Spectral properties of multiorder diffractive lenses. *Applied Optics*, 34, 14 (may 1995), 2462-2468.

[3] Davies, H., *Proc. Inst. Elec. Engrs.,* Vol 101, (1954), p.116